



**UNIVERSITA' DI NAPOLI "FEDERICO II"**

**DOTTORATO DI RICERCA  
BIOCHIMICA E BIOLOGIA MOLECOLARE E CELLULARE  
XXIII CICLO**

***Structural characterization of recombinant human  
gastrokine-1: biochemical properties of the purified protein***

**Candidate  
Paolo Mallardo**

Tutor  
Prof. Paolo Arcari

Coordinator  
Prof. Paolo Arcari

Co-Tutor  
Dr. Emilia Rippa  
Dr. Luigi Michele Pavone

**Academic Year 2010/2011**

---

## RINGRAZIAMENTI

La lista di quanti mi hanno accompagnato in questo splendido ed a volte accidentato percorso è sicuramente lunga...

Il principale ringraziamento va al Prof. Arcari che, oltre a contribuire alla mia formazione professionale, è riuscito, attraverso una relazione didattica prevalentemente di poche parole ad insegnarmi quanto sia più importante mettersi all'ascolto dell'altro piuttosto che parlare sempre e semmai parlare a vuoto; infatti si dice che il saggio parla quando è interrogato e penso che mia fortuna è stata aver incontrato una persona sapiente!

Ringrazio, inoltre, la Dott.ssa Rippa. Come non dimenticare, forse un po' anche nostalgicamente, le lunghe ed interminabili giornate trascorse tra scienza (continui e ripetuti esperimenti) e vita (materni e profondi consigli nei momenti di scoraggiamento). Da non dimenticare anche, le belle litigate che sicuramente hanno contribuito a fortificare la mia persona umana e professionale.

Umanità, professionalità e tanto calore, queste son le caratteristiche che animano le persone (dai professori agli studenti) del VI° piano della torre biologica. È stato un luogo dove sono veramente cresciuto e vi devo veramente tanto! Ringraziamenti di cuore vanno al Prof. Masullo, mente pratica del nostro laboratorio e persona sempre disponibile ad ogni problema, al Prof. De Vendittis, alla Dott.ssa Lamberti, Dott.ssa Ruocco e Dott. Rullo, sempre pronti a darmi buoni consigli. Lo staff col quale ho lavorato (Dott.ssa Altieri, vera amica e collega di lavoro e la piccola Stellina, mia sorella minore). Ed a quanti (non li elenco tutti altrimenti si fa notte) hanno compiuto questo percorso con me nella grande famiglia del VI° piano, Grazie di cuore!

Infine, un ringraziamento va al Dott. Pavone che, particolarmente nella fase ultima, ha contribuito fortemente, prima come ricercatore e poi come amico alla stesura della mia tesi.

Dovrei ringraziare (tanto lo sanno!) tante altre persone che in un modo o nell'altro mi hanno accompagnato in questa bella avventura.

Voglio concludere riportando la frase di un filosofo inglese (W. James), il quale scriveva che: *“L'uso migliore della vita è di spenderla per qualcosa che dura più della vita stessa”*.

Questa frase racchiude un po' quello che sono, penso e che cerco di essere, ogni giorno, per gli altri. Grazie a tutti!



---

## SUMMARY

Gastric cancer (GC) is one of the most leading cause of cancer death. The high mortality is due to late diagnosis, although the gastric infection by *Helicobacter pylori* represents one of the most significant risk factors for this type of cancer. Gastrokine-1 (GKN1) is expressed in normal gastric tissue, while it is scarcely present in samples from patients infected by *H. pylori*, and completely absent in GC tissues and cell lines. Therefore, GKN1 could be a potential marker for GC diagnosis and a possible tumor suppressor. In order to get more insights into the molecular mechanisms on the pathology of GC, this study was directed to better understand the structural features and the biological activity of this protein. In details, this study was directed to: 1) synthesis of recombinant mature GKN1 by cloning, expression and purification; 2) characterization of structural and biochemical properties of recombinant GKN1 by circular dichroism, fluorescence spectroscopy, and limited proteolysis; 3) evaluation of the effect of recombinant GKN1 on gastric cancer cell lines growth; 4) construction of a 3D structural model of the protein. The first protocol for biosynthesis and purification of native human GKN1 in the homologous expression system of *Pichia pastoris* was settled. The use of biochemical analytical methods such as limited proteolysis led to the identification of exposed amino acid residues on the protein surface. The resistance of GKN1 to the action of proteolytic enzymes was somehow explanatory of its stability in the harsh stomach environment. Spectroscopic studies (fluorescence and circular dichroism) showed that the protein is endowed by a non-proper globular structure due probably to the presence of two domains. These domains showed a different behaviour toward chemical and physical denaturant. The results well correlate with predicted GKN1 secondary structure and 3D structure model. Finally, the recombinant protein showed anti-proliferative properties on gastric cancer cell lines. Our findings contribute to a preliminary clarification of the role of GKN1 in the pathogenesis of gastric cancer.

---

## RIASSUNTO

Il carcinoma gastrico (GC) è una delle principali cause di morte per cancro. L'elevata mortalità è dovuta ad una diagnosi tardiva, anche se l'infezione da *Helicobacter pylori* (*H. pylori*) rappresenta uno dei fattori di rischio più significativi. La Gastrokine-1 (GKN1) è espressa nel tessuto gastrico normale, mentre è scarsamente presente nei pazienti con infezione da *H. pylori*, ed è completamente assente in tessuti di pazienti affetti da GC. Pertanto, GKN1 potrebbe rappresentare un potenziale "marker" per l'individuazione in fase precoce della malattia ed un possibile farmaco soppressore tumorale. Allo scopo di ottenere informazioni preliminari sui meccanismi molecolari alla base del GC, questo lavoro di tesi è rivolto alla comprensione delle caratteristiche strutturali e funzionali della GKN1.

Nel dettaglio, questo studio è stato sviluppato come di seguito riportato: 1) sintesi ricombinante di GKN1 mediante clonaggio, espressione e purificazione; 2) caratterizzazione delle proprietà strutturali e biochimiche di GKN1 ricombinante attraverso studi di dicroismo circolare, fluorescenza e proteolisi limitata; 3) valutazione dell'effetto di GKN1 ricombinante sulla vitalità di linee cellulari di cancro gastrico 4) costruzione di un modello strutturale 3D della proteina. Il protocollo impiegato per la biosintesi e la purificazione di GKN1 umana si basa sull'utilizzo del sistema di espressione eucariotico di lievito *Pichia pastoris* (*P. pastoris*). L'utilizzo di metodi biochimici analitici come la proteolisi limitata ha portato all'individuazione di residui di aminoacidi esposti sulla superficie della proteina. La resistenza di GKN1 all'azione di enzimi proteolitici è, in qualche modo, esplicativa della sua stabilità nell'ambiente gastrico. Studi spettroscopici di fluorescenza e di dicroismo circolare hanno dimostrato che la proteina non ha una struttura globulare compatta, ma sembra caratterizzata dalla presenza di due domini. Questi domini presentano un diverso comportamento chimico e fisico verso gli agenti denaturanti. I dati ottenuti risultano coerenti con le informazioni di struttura secondaria predetti per GKN1 e con il modello 3D. Infine, la proteina ricombinante ha mostrato proprietà anti-proliferative su linee cellulari di cancro gastrico. I nostri risultati contribuiscono al chiarimento preliminare del ruolo del GKN1 nella patogenesi del cancro gastrico.

## INDEX

	<b>Pag.</b>
<b>1. INTRODUCTION</b>	<b>1</b>
1.1 Gastric cancer	1
1.2 Gastrokine-1	2
1.3 Scientific hypothesis and aim of the work	3
<b>2. MATERIALS AND METHODS</b>	<b>5</b>
2.1 Microorganisms and culture media	5
2.2 Vector construction and <i>P. pastoris</i> cell transformation	5
2.3 GKN1 expression and purification	6
2.4 Mass spectrometry	7
2.5 Limited proteolysis	8
2.6 Western blotting	8
2.7 CD and fluorescence spectroscopy	8
2.8 Cell culture	9
2.9 Cell viability assay	10
<b>3. RESULTS</b>	<b>11</b>
3.1 Expression and purification of recombinant GKN1	11
3.2 Primary structure and proteolytic sites of recombinant GKN1	11
3.3 Fluorescence measurements	19
3.4 Circular dichroism measurements	23
3.5 GKN1 secondary structure prediction and 3D modelling	29
3.6 Biological activity of GKN1	29

*Contents*

---

	<b>Pag.</b>
<b>4. DISCUSSION/CONCLUSIONS</b>	<b>33</b>
<b>5. REFERENCES</b>	<b>39</b>

<b>LIST OF TABLES AND FIGURES</b>		<b>Pag.</b>
<b>Table 1.</b>	<b>Calculated Secondary Structure Fractions in GKN1</b>	<b>23</b>
<b>Figure 1.</b>	<b>Purification of GKN1</b>	<b>12</b>
<b>Figure 2.</b>	<b>Proteolysis of GKN1 with trypsin</b>	<b>13</b>
<b>Figure 3.</b>	<b>Proteolysis of GKN1 with chymotrypsin</b>	<b>15</b>
<b>Figure 4.</b>	<b>Proteolysis of GKN1 with thermolysin</b>	<b>16</b>
<b>Figure 5.</b>	<b>Western blot of GKN1 proteolysis with trypsin, chymotrypsin and thermolysin</b>	<b>17</b>
<b>Figure 6.</b>	<b>Schematic representation of GKN1 proteolytic sites</b>	<b>18</b>
<b>Figure 7.</b>	<b>Proteolysis of GKN1 in absence and presence of DTT</b>	<b>20</b>
<b>Figure 8.</b>	<b>Denaturation profile of GKN1 in guanidine-HCl</b>	<b>21</b>
<b>Figure 9.</b>	<b>Denaturation profile of GKN1 in urea</b>	<b>22</b>
<b>Figure 10.</b>	<b>Denaturation profile of GKN1 in non-denaturing conditions</b>	<b>24</b>
<b>Figure 11.</b>	<b>CD spectra of GKN1 in the far UV</b>	<b>25</b>
<b>Figure 12.</b>	<b>CD spectra of GKN1 in the near UV</b>	<b>27</b>
<b>Figure 13.</b>	<b>Differential scanning calorimetry (DSC) of GKN1</b>	<b>28</b>
<b>Figure 14.</b>	<b>Secondary structure of GKN1 predicted by Psipred Server</b>	<b>30</b>
<b>Figure 15.</b>	<b>3D model of GKN1 built at the Tasser Bioinformatic Server</b>	<b>31</b>
<b>Figure 16.</b>	<b>Effect of GKN1 on cell growth</b>	<b>32</b>
<b>Figure 17.</b>	<b>Schematic representation of the two possible unfolding pathways in Gdn-HCl and urea solution for human GKN1</b>	<b>35</b>

*Contents*

---

## **INTRODUCTION**

### **1.1 Gastric cancer**

Gastric cancer (GC) is one of the most common solid tumor in the world. High incidence rates are found in Japan, in some regions of East Asia and in some Latin American countries (1-2), but the rates of mortality and incidence of the disease are very high also in Europe. Despite advances in conventional therapies, the survival rate of patients with GC up to 5 years is poor (<30%), thus GC resulting the third leading cause of death after lung, colorectal and breast cancer (3). The incidence of GC is often related to advancing age: in particular, the tumor occurs on average between 45 and 55 years and affects males twice than females.

The aetiology of GC is multi-factorial including environmental, genetic and infectious factors (2, 4-6). A prominent role is played by environmental factors such as smoking and alcohol abuse, presence of carcinogen agents in some foods, a diet rich of fat, smoked or salted foods and missing of fruits and vegetables, and finally, exposure to carcinogenic environmental contaminants (4). The influence of genetic factors in gastric carcinogenesis has been documented by studies where the occurrence of more than one case of GC in the same family is associated to a genetic predisposition due to alteration in the tumor suppressor genes p53 and APC (adenomatous *polypis coli*) which are involved in the malignant transformation of various organs (5). Multiple evidence demonstrated the important role of *Helicobacter pylori* (*H. pylori*) infection in the development of GC (6-8). *H. pylori* is a parasite of the gastric mucosa and induces a complex inflammatory reaction characterized by the release of inflammatory cytokines and production Reactive Oxygen Species (ROS) (6). These factors created to fight the infection of *H. pylori* also damage the cells of the stomach when they do not possess sufficient reserves of natural antioxidants such as vitamin C or vitamin E. Thus, most of *H. pylori* infected subjects develop acute gastritis, which, if not properly treated, causes chronic disease, and evolves in ulcer or tumor (9).

In two-thirds of patients in western countries, GC is diagnosed in an advanced stage, and because this type of tumor is resistant to radiotherapy and chemotherapy, surgery represents the only curative treatment,

although often it is only a temporary solution (10). Currently, therefore, there is an urgent need to clarify the molecular mechanisms underlying the processes of transformation and neoplastic progression, to identify new prognostic parameters and to develop more effective therapies for GC.

Recently, the tissue-specific protein gastrokine-1 (GKN1) has emerged as a possible biomarkers for GC (11-12). This protein expressed in the human stomach of healthy individuals, is absent in gastric adenocarcinoma tissues, and in other tissues such as placenta and ovaries (13-15). However, GKN1 might also be present at low levels in normal uterus, liver, kidney, pancreas and adrenal and salivary glands (12). Some evidence suggests that GKN1 is involved in filling the lumen of the surface layer of epithelial cells to maintain the integrity of the mucosa and to regulate cell proliferation and differentiation (12-13). As result of the damage to the gastric mucosa, the presence of GKN1 helps to restore the normal state of the mucosa (14). On the contrary, if the protein is not expressed, the repair process is impeded. Addition of GKN1, in fact, promotes restoring of damaged epithelium in gastrointestinal cells (16). It has been also demonstrated that GKN1 expression induces apoptosis in GC cells, demonstrating the importance of GKN1 in inhibiting the development of GC (17). Individuals with a lower expression of the protein have an increased risk to develop gastric diseases (18). The protein is, in fact, not expressed in samples from patients infected with *H. pylori* and is completely absent in tissues of GC (11-12, 14-15).

### 1.2 Gastrokine-1

Gastrokine-1 protein, previously known as 18 kDa antrum mucosal protein (AMP-18) was subsequently called by "Human Gene Nomenclature Committee" GKN1 for its tissue-specific expression and its highly conserved presence in the gastric mucosa of many mammals species (12-13). The gene coding for GKN1 (*CA11*) (accession number: BK0017373), is located on chromosome 2 (19). Sequence analysis of the gene showed that the human transcript contains two potential translation start sites (ATG). The first start codon would generate a protein of 199 amino acids whereas the second ATG, located 42 bp downstream, would

make a protein of 185 amino acids. Among the two starting sites, the second appears more possible since it contains a Kozak sequence (GCAGCCAACATG) (20). Comparison of the translated amino acid sequence of human GKN1 with that of other species showed homology only after the second ATG, and its product is predicted to be of 18 kDa. In addition, amino acid sequencing of native GKN1 from pig and N-terminal Edman's degradation of native human GKN1 confirmed that the protein was made of 185 amino acids containing a 20 amino acids extracellular signal peptide localized in the N-terminal region (13-14). The protein contains a conserved central structural BRICHOS domain (21) of about 100 amino acids containing two conservative cysteine residues that are possibly involved in intra- and/or inter-molecular disulfide bridges. The putative association of GKN1 with such domain structure, and with at least three different possible functions, has been proposed, but not yet been conclusively demonstrated. In fact, the BRICHOS domain has been found in proteins with a wide range of functions and disease associations (22-23). There are 8 known families including the cancer associated GKN1, GKN2 and LECT1, the three dementia associated ITM2 families, the respiratory disease associated proSP-C, and TNMD. Among these protein families there is a little sequence identity, the proteins are generally cleaved to produce their active forms, and there are no 3D structures in the PDB database even for remote homologue proteins. This protein represents a promising tumor marker that could be highly useful in early diagnosis and development of new drug therapies for GC.

### **1.3 Scientific hypothesis and aim of the work**

Although GKN1 seems to play an important role in the turnover of epithelial cells, in maintaining the integrity of the mucosa and in the processes of cell proliferation and differentiation, a full characterization of its structure and biological activity is still lacking. The aim of the thesis work was to characterize the structural and functional properties of GKN1. Since the purification of the protein from human tissues (normal human antrum mucosa) resulted very difficult due to the unavailability of human specimens, a recombinant production protocol using the

## *Introduction*

---

homologous expression system of *Pichia pastoris* was settled. The production of a recombinant GKN1 allowed its chemical-physical and biochemical characterization by using spectroscopic and biochemical techniques. Bioinformatics tools were used for a prediction of a three-dimensional modelling of the protein. Finally, the recombinant protein was also tested for its biological activity in the regulation of cellular viability. This recombinant GKN1 could be also useful for crystallization trials directed toward the resolution of its 3D structure.

## MATERIALS AND METHODS

### 2.1 Microorganisms and culture media

*Escherichia coli* (*E. coli*) JM109 strain was purchased from Boehringer and used for genetic manipulation. Culture medium for *E. coli* was LB (Luria-Bertani) liquid and solid (agar), prepared as described by Sambrook et al. (24). *Pichia pastoris* (*P. pastoris*) GS115 strain was purchased from Invitrogen and used as recombinant protein expression system. Culture media for *P. pastoris* were Buffered Minimal Glycerol (BMGY, 100 mM potassium phosphate, pH 6.0, 1.34% yeast nitrogen base (YNB), 0.002% biotin, 1% glycerol), and Buffered Minimal Methanol (BMMY, 100 mM potassium phosphate, pH 6.0, 1.34% YNB, 0.002% biotin, 0.5 % methanol). Ampicillin (Amp) was purchased from Sigma and used at a concentration of 1 mg/ml for both bacterial and yeast cultures.

### 2.2 Vector construction and *P. pastoris* cell transformation

pCDNA3.1 containing the GKN1 cDNA (pCDNA3.1/GKN1) (14) was used as a template for PCR amplification. The following primers were used:

PIC-GKF1 (forward) 5'TACGTAATGAAGTTCACAATTGTCTT3'  
corresponding to M1KFTIVF of full length GKN1;

PIC-GKF2 (forward) 5'TACGTAAACTATAATATCAACGTCAAT3'  
corresponding to the Y2NYNINVN sequence of mature GKN1  
(truncated of the first 20 leader amino acids);

PIC-GKR1 (reverse) 5'GCGGCCGCTCAATGGTGATGGTGATG3'  
corresponding to the (His)6 C-terminal region of the pCDNA3.1/GKN1  
construct.

The first two primers contained SNAB1 restriction sites and the last contained NOT1 site, respectively. The PCR (GKN1A and GKN1B) products were then cloned in pPIC9K digested with the same restriction enzymes, and the isolated positive clones were sequenced (pPIC9K/GKN1).

*P. pastoris* (strain GS115) competent cells were prepared as it follows:

cells were inoculated into 10 ml of Yeast Peptone Dextrose Medium (YPD, Invitrogen) and grown overnight at 30 °C in a shaking bath. Subsequently, the inoculum was diluted in 100 ml of YPD to a starting cell concentration of 0.1 OD<sub>660nm</sub>. 100 ml of culture were grown at 30 °C to a concentration of 0.7 OD<sub>660nm</sub>. Cell culture was harvested by centrifugation at 4500 rpm for 20 min, and washed in 50 ml of solution A [1 M sorbitol (Fisher), 10 mM bicine (Sigma), pH 8.35, 3% (v:v) ethylene glycol (Merck)]. Cells were re-suspended in 4 ml of solution A, and divided into aliquots of 0.2 ml in sterile Eppendorf tubes of 1.5 ml. 10 ml of DMSO were added in each aliquot. Competent cells were frozen at -80 °C. *P. pastoris* competent cells were transformed according to the following procedure. 50 mg of pPIC9K/GKN1, linearized with SAL1, in a final volume of 20 ml were used. The DNA was added to competent cells still frozen together with salmon sperm (Sigma) as DNA carrier. The sample was incubated at 37 °C in a water bath for 5 min under shaking. 1.5 ml of solution B [40% (w:v) polyethylene glycol 1000 (Sigma), bicine 0.2 M, pH 8.35] were added to the samples that were incubated for 1 h at 30 °C, centrifuged at 3000 rpm for 10 min and re-suspended in 1.5 ml of solution C (0.15 m NaCl, 10 mM bicine, pH 8.35). After a final centrifugation, the pellet was re-suspended in 0.2 ml of solution C. The cells were plated on agarose plates containing selective His<sup>-</sup> culture medium (Invitrogen), and grown for 2 days at 30°C.

### **2.3 GKN1 expression and purification**

Analytical expression was first carried out to identify best expressing GKN1 clone. *P. pastoris* transformed colonies were inoculated into 10 ml of BMMY. The culture was incubated at 30°C by vigorous shaking for 72 h. Cells were then harvested by centrifugation at 3500 rpm for 15 min at 4 ° C, and the supernatant of each clone was analyzed by SDS-PAGE electrophoresis and Western blotting using mouse monoclonal anti-GKN1 antibody (clone 2E5, Abnova). GKN1A was not expressed. In contrast, the mature form of the protein, GKN1B, was expressed in all clones examined. The clone showing the high GKN1 expression (clone 27) was grown, and stored at -80°C. Preparative GKN1 expression was performed in 2 l of culture medium. Briefly, 100 ml of *P. pastoris* clone

27 were inoculated in 12 ml of BMGY, and grown overnight at 30°C. 3 ml of this culture were then used to inoculate 500 ml of BMGY and grown overnight up to a cell concentration of 5 OD<sub>600nm</sub>. Cells were harvested by centrifugation, re-suspended in a volume of 2 l of BMMY, and grown for 72 h at 30°C under vigorous shaking. After the first 24 h, methanol (0.5% final concentration) was added to the growing culture every day. Finally, cells were harvested by centrifugation at 8000 rpm for 40 min, and the resulting supernatant was cleaned using 0.22 mm filters, and stored at 4 °C.

Proteins from supernatant were precipitated with 70% ammonium sulfate (844 g/2 l) at 4°C, centrifuged at 13000 rpm for 50 min, and the resulting pellet was re-suspended in 50 ml of buffer A (50 mM TrisHCl, pH 8.5). The protein sample was then dialyzed against 2 l of buffer A, and applied on anion exchange DEAE Sepharose (1x60 cm) (FF, Pharmacia Biotech). The column, equilibrated at 4 °C in buffer A, was washed with 10 x volumes column, and eluted with a linear gradient (0 - 500 mM NaCl) at a flow rate of 2 ml/min (total volume: 10x column volume). The elution profile was followed at 280 nm, and fractions (12 ml) were then analyzed by SDS-PAGE. Fractions containing GKN1 were pooled, dialyzed against buffer A, and applied on a Ni-NTA Agarose column (10 ml). After washing the column with buffer A (10x column volume), the column was washed with 5x column volume of buffer A containing 5 mM imidazole, and subsequently the protein was eluted with buffer A containing 100 mM imidazole. Fractions were analyzed by SDS-PAGE and Western blotting, and those fractions containing purified GKN1 were pooled, dialyzed against buffer A or 20 mM phosphate buffer pH 7.0, and stored at -20°C. Protein concentration was determined according to Lowry method (25).

## **2.4 Mass spectrometry**

GKN1 was analyzed on a C8 column by High Performance Liquid Chromatography (HPLC) coupled with a LCMS EV 2010 Liquid Chromatography Mass Spectrometer (Shimadzu). Sample (30 µl) was first eluted at 0.5 ml/min with a liner gradient from 5 to 40% acetonitrile (Romil) in water containing 0.1% TFA (trifluoroacetic acid) (Applied

Biosystems) in 50 min, and then from 40 to 95% acetonitrile in water containing 0.1% TFA, in 20 min.

## **2.5 Limited proteolysis**

The limited proteolysis experiments were performed on purified GNK1 in phosphate buffer at pH 7.0. 100 µg of protein were digested by 10 µg trypsin, chymotrypsin in native conditions or denaturing conditions in presence of 100 mM DTT (dithiothreitol). The digested products were analyzed on denaturing and non-denaturing gels (without boiling the protein samples and without adding β-mercaptoethanol) by coomassie blue staining. Bands from the gel were then eluted for N-terminal sequencing by Edman's degradation according to a standard procedure.

## **2.6 Western blotting**

Western blotting was performed according to standard procedure. Generally, proteins were separated by SDS-PAGE, electro-transferred to PVDF membrane, and incubated for 1 h at room temperature with anti-GKN1 antibody, at dilution of 1:500. Anti-mouse secondary antibody conjugated with horse radish peroxidase (HRP) (Sigma) was used at a dilution of 1:20.000. The specific protein was visualized by a enhanced chemiluminescence detection reagents (SuperSignal West Pico), and exposed to X-ray film. All films were analyzed by using Image J software.

## **2.7 CD and fluorescence spectroscopy**

Sample solutions for spectroscopic measurements were prepared in 20 mM NaP buffer at pH 8.5, and the protein concentration was determined by UV spectra using a theoretical, sequence-based (26), extinction coefficient of  $30680 \text{ M}^{-1} \text{ cm}^{-1}$  at 280 nm. CD spectra were recorded with a Jasco J-715 spectropolarimeter equipped with a Peltier type temperature control system (Model PTC-348WI). Molar ellipticity per mean residue,  $[\vartheta]$  in  $\text{deg cm}^2\text{dmol}^{-1}$ , was calculated from the equation:  $[\vartheta] = [\vartheta]_{\text{obs}} \text{mrw}/10 \cdot l \cdot C$ , where  $[\vartheta]_{\text{obs}}$  is the ellipticity measured in

degrees,  $m_r$  is the mean residue molecular weight, (113.3Da) for GKN1 protein,  $C$  is the protein concentration in  $\text{g/mL}^{-1}$  and  $l$  is the optical path length of the cell in cm. CD spectra were recorded by using 0.1 and 0.5 cm path length cells in the far-UV and near-UV region, respectively. They were recorded at 20°C with a time constant of 4 s, a 2 nm bandwidth and a scan rate of 20 nm/min, signal-averaged over at least three scans, and baseline corrected by subtracting a buffer spectrum. Spectra were analyzed for secondary structure amount according to the CDSSTR method (27) using Dichroweb (28-29). The thermal unfolding curves were recorded in the temperature mode, by following the change of the CD signal at 216nm and at 290nm with a scan rate of 1.0°C/min. The temperature-induced denaturation of GKN1 protein was found to be irreversible and therefore not allowing us to perform the thermodynamic analysis of denaturation curves.

Fluorescence spectra were recorded at 25°C on a computer assisted Cary Eclipse spectrofluorimeter (Varian) at a scan rate of 60 nm/min using an excitation wavelength of 280 nm; excitation and emission slits were set to 10 nm. The fluorescence spectrum was measured in the range 300-450 nm. The denaturation with guanidinium chloride (Gdn-HCl) was performed using concentrations of 3 M and 6.3 M Gdn-HCl, and then the fluorescence spectrum was recorded.

## **2.8 Cell culture**

Human gastric cancer cell, AGS, human epidermal pulmonary carcinoma cell, H1355 and embryonic kidney cell HEK293 lines were grown in DMEM-F12 (Dulbecco's modified Eagle medium, Cambrex) supplemented with heat inactivated Fetal Bovine Serum (FBS), 100 U/ml penicillin, 100 mg/ml streptomycin, 1% L-glutamine at 37°C in a 5% CO<sub>2</sub> atmosphere. The cells were harvested by treatment with 0.25% trypsin, EDTA 0.02M in PBS pH 7.2, washed with culture medium and re-suspended in complete growth medium. The cells were maintained in culture for no more than two weeks.

## **2.9 Cell viability assay**

Cell proliferation was assessed by measuring the reduction of 3-(4,5-dimethylthiazol-2-yl)-2,5-diphenyltetrazolium bromide (MTT) to formazan salts by the enzyme succinate dehydrogenase.

In this colorimetric assay, the activity of mitochondrial succinate dehydrogenase, active only in living cells, which cuts the tetrazole ring of MTT (yellow substance) with the formation of formazan (a blue salt) is measured. This reaction is evaluated by spectrophotometric reading of the sample at a wavelength of 570 nm. Re-suspended cells (about 7500 cells/well) were plated in 96-well plates and exposed to increasing concentrations of GKN1 ( $10^{-4}$ ,  $10^{-5}$ ,  $10^{-6}$ ,  $10^{-7}$  M) for different time intervals (24, 48 and 72 h). Subsequently, the MTT solution (5 mg/ml) in PBS was added to the wells, and the plates were incubated for 2 h at 37°C. The reaction was stopped by removing the supernatant followed by the dissolution of the formazan product by the addition of 150  $\mu$ l of isopropanol. The absorbance at 570 nm was determined using a Bio-Rad ELISA reader. Cell proliferation was expressed as the percentage of formazan formation in the samples treated with the substances compared to the negative control treated with only solvent.

## RESULTS

### 3.1 Expression and purification of recombinant GKN1

*P. pastoris* expression vector pPIK9K, methanol inducible, containing GKN1 cDNA encoding mature protein was used to transform GS115 yeast strain. The expressed recombinant GKN1 protein, secreted into culture medium, was identified after ammonium sulfate precipitation (70%) by mass spectrometry coupled to HPLC. As reported in Fig. 1A, HPLC chromatogram showed a peak of GKN1 accounting of about 2% of total proteins. The peak was collected, and the presence of GKN1 was confirmed by electrospray mass spectrometry analysis. Following ammonium sulfate precipitation, GKN1 was further purified by DEAE and Ni-NTA chromatography. Fig. 1B shows the DEAE chromatogram of GKN1 eluted with a linear salt gradient. Fractions containing the recombinant protein were analyzed by SDS-PAGE (Fig. 1C), and the appropriate pooled fractions were separated on Ni-NTA agarose chromatography. The Ni-NTA elution profile is reported in Fig. 1D. Finally, the purified protein was concentrated up to about 2-3 mg/ml and stored in 20 mM phosphate buffer, pH 7.4 at  $-20^{\circ}\text{C}$ . Fig. 1E reports SDS-PAGE electrophoretic profile of the purified GKN1. The total amount of GKN1 purified from 1 liter of culture medium was around 40 mg as evaluated by Lowry method.

### 3.2 Primary structure and proteolytic sites of recombinant GKN1

Purified GKN1 was analyzed by limited proteolysis using trypsin, chymotrypsin and thermolysin proteases. From the SDS-PAGE electrophoretic profile of the time course of time-dependent trypsin cleavage of GKN1 two major fragments of about 17 and 11 kDa were detected (Figure 2A). The formation of proteolytic products was accompanied by the disappearance of intact recombinant GKN1 (Fig. 2B). Edman's degradation of the largest protein fragment (17 kDa) allowed to establish the N-terminal sequence of the intact protein thus indicating the presence of a proteolytic cleavage site toward the C-terminal, whereas the sequence of 11 kDa fragment showed the presence of a proteolytic site at the level of Lys91 (numbering mature GKN1).

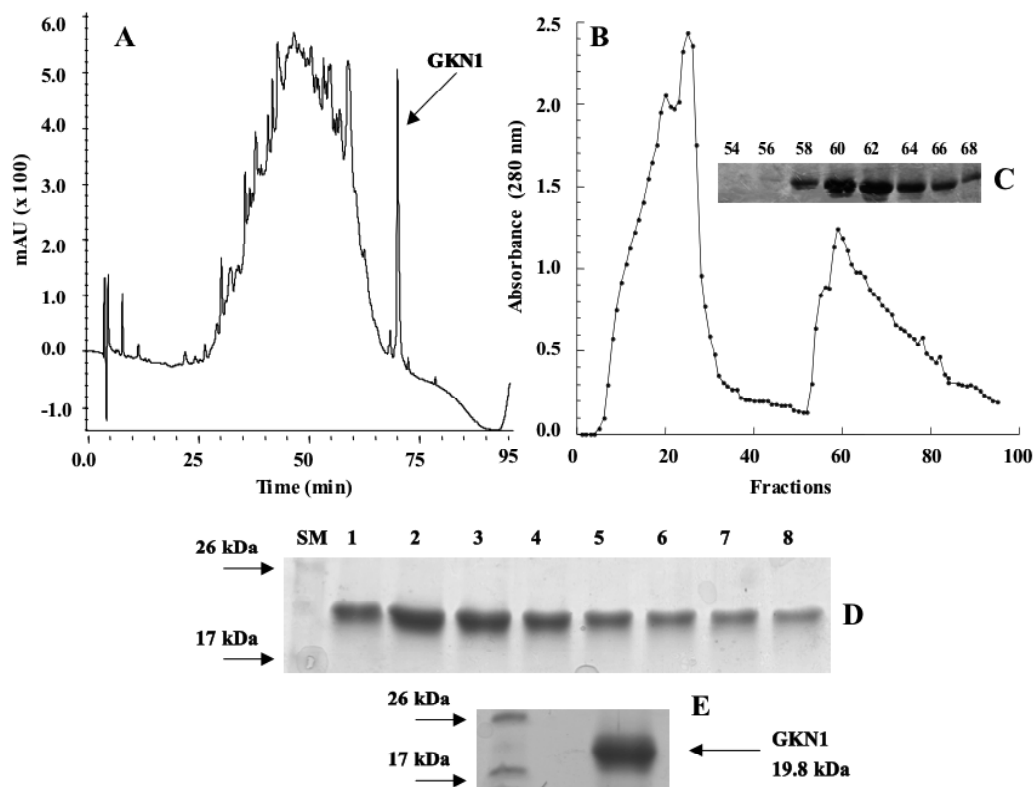


**Figure 1 Purification of GKN1**

A. HPLC of culture medium. B. DEAE chromatography after ammonium sulphate precipitation. C. SDS-PAGE of DEAE fraction containing GKN1. D. SDS-PAGE of Ni-NTA chromatography elution profile of the pool after DEAE fractions. E. SDS-PAGE of the purified GKN1

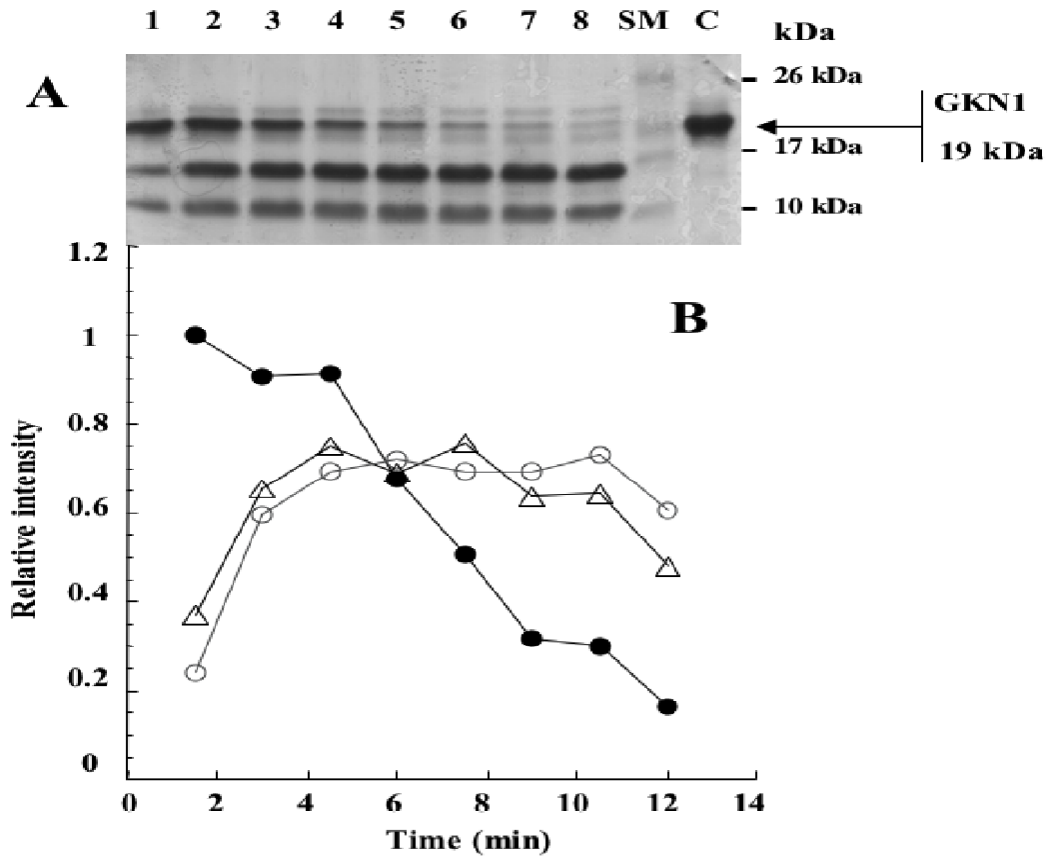


**Figure 2 Proteolysis of GKN1 with trypsin**

A. GKN1 was incubated in the presence of trypsin and at the indicated times, sample aliquots were withdrawn from the reaction mixture and separated on SDS-PAGE. Lanes: 1 – 8 samples after 1.5, 3.0, 4.5, 6.0, 7.5, 9.0, 10.5, 12.0 minutes incubation; SM, size marker; C, control intact GKN1. B. Densitometric evaluation of the band intensity.

Limited proteolysis of the protein with chymotrypsin yielded the formation of three major peptides of about 15, 10 and 5 kDa (Fig. 3). The N-terminal sequence of the 15 kDa fragment started at level of Tyr4 therefore, there must be a further proteolytic cleavage site at the C-terminal region of the protein.

The N-terminal sequence of the 10 kDa fragment indicated the presence of a cleavage site at level of Phe141. Also in this case the molecular weight of this fragment suggests the presence of an additional cleavage site at the C-terminal. The third 5 kDa fragment gave two different N-terminal sequences indicating the presence of two proteolytic sites at levels of His66 and Tyr103. Also for these two fragments, their sizes suggests the presence of an additional cleavage site at the C-terminal.

Following the digestion of GKN1 with thermolysin, four fragments of about 18, 16, 11 and 9 kDa were observed by SDS-PAGE (Fig. 4A). The first two fragments showed the same N-terminal sequences indicating that both fragments were obtained by cleavage of GKN1 at position of Asn5 and at two different cleavage positions in the C-terminal region of the protein. The fragment of 11 kDa produced two N-terminal sequences that indicated cuts at level of Lys87 and Phe141. On the bases of the sizes of these two fragments, the presence of an additional cleavage site at the C-terminal was supposed. From the 9 kDa band three fragments were generated corresponding to cleavages at level of Lys87, Phe141 and Phe142. Also in this case, additional cleavage sites are present at the C-terminal region of each fragment.

To assess the region of GKN1 that is recognised by GKN1 antibody, the protein was cleaved by proteases and the digestion products were analyzed by Western blotting. When trypsin and chymotrypsin were used, the antibody recognized the largest proteolytic fragment whereas it recognized the 16 kDa fragment of thermolysin digestion (Fig. 5). These results suggested that the epitopic region of the protein recognized by the mouse monoclonal antibody anti-GKN1 is located within the first 60 amino acid residues of the protein. A schematic representation of the recombinant GKN1 primary structure and of proteolytic sites is reported in Fig. 6.

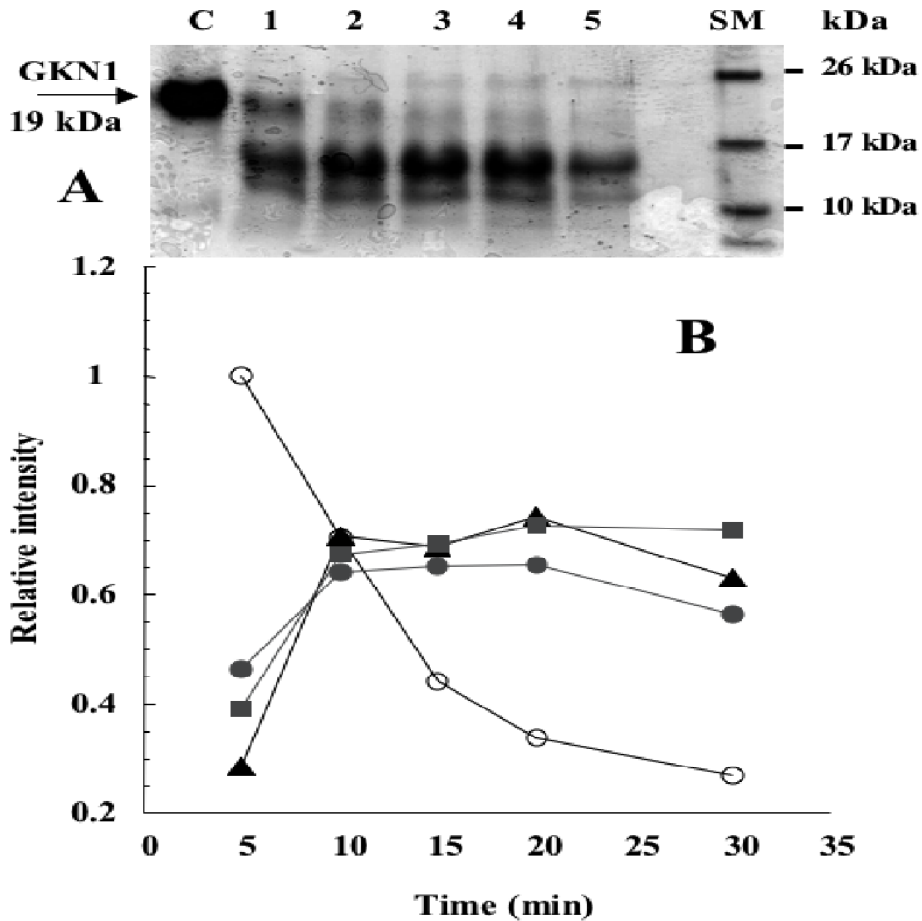


### Figure 3 Proteolysis of GKN1 with chymotrypsin

A. GKN1 was incubated in the presence of chymotrypsin and at the indicated times, sample aliquots were withdrawn from the reaction mixture and separated on SDS-PAGE. Lanes: C, control intact GKN1; 1 – 5 samples after 5, 10, 15, 20, 25 minutes incubation; SM, size marker. B. Densitometric evaluation of the band intensity.

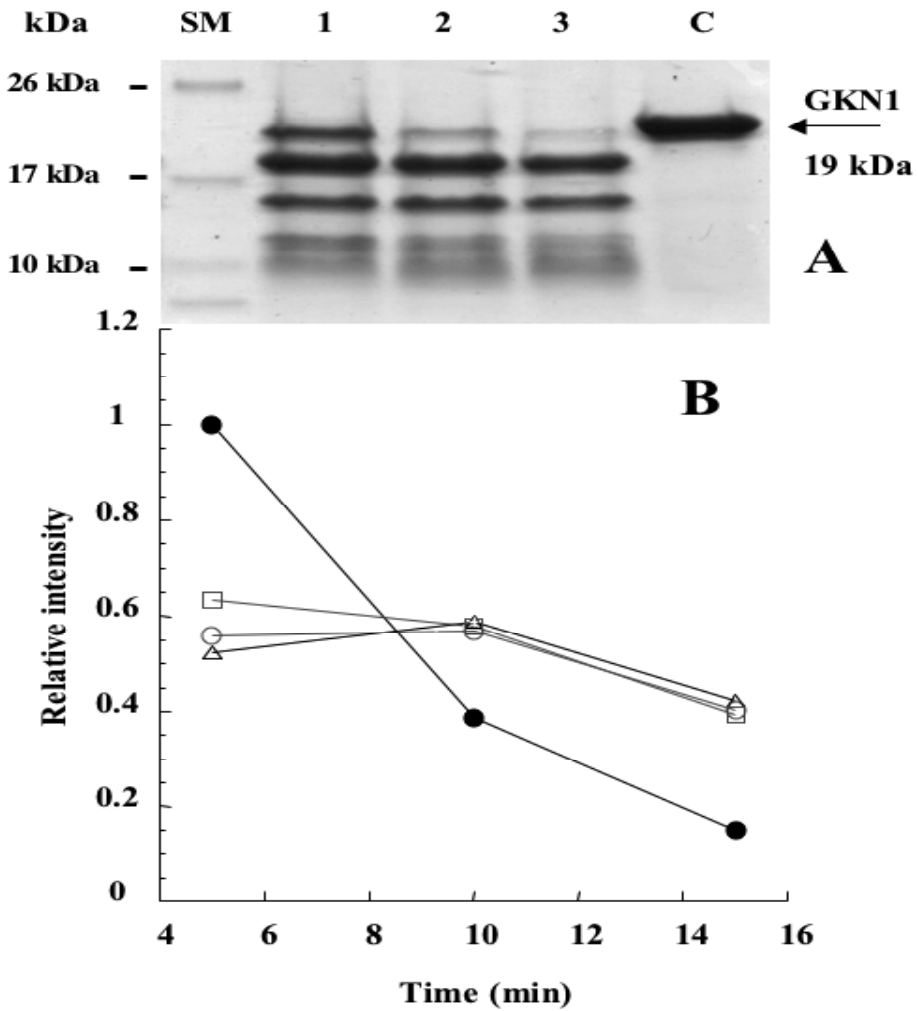


**Figure 4 Proteolysis of GKN1 with thermolysin**

A. GKN1 was incubated in the presence of thermolysin and at the indicated times, sample aliquots were withdrawn from the reaction mixture and separated on SDS-PAGE. Lanes: SM, size marker; 1 – 3 samples after 5, 10, 15 minutes incubation; C, control intact GKN1. B. Densitometric evaluation of the band intensity.

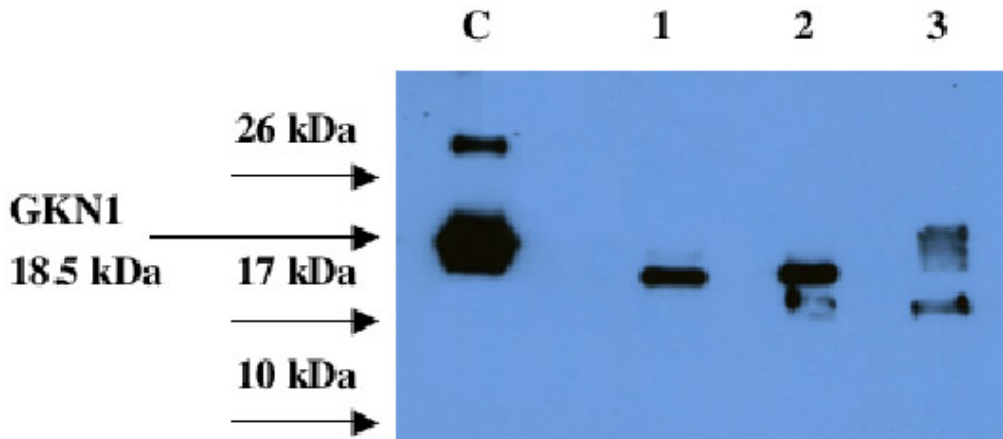


**Figure 5 Western blot of GKN1 proteolysis with trypsin, chymotrypsin and thermolysin**

C, control intact GKN1. Lane 1, 2 and 3 GKN1 after digestion with trypsin, chymotrypsin and thermolysin, respectively.

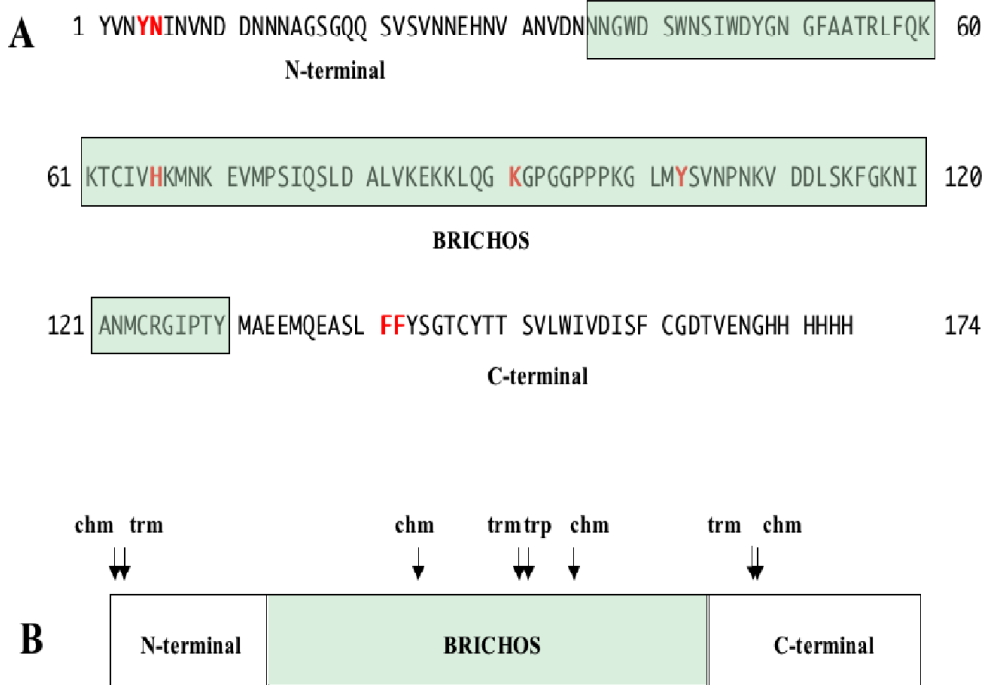


**Figure 6 Schematic representation of GKN1 proteolytic sites**

A. Amino acid sequence of recombinant His tagged GKN1 showing the region containing the BRICHOS domain. B. Schematic representation of proteolytic sites. Chm, Chymotrypsin; trm, Thermolysin; trp, Trypsin.

From these results emerged that a trypsin proteolytic site was located at the level of Lys91 in a region of the protein comprised between the first Cys (Cys63) and the other three Cys (Cys124, Cys147 and Cys161). To test whether these two cysteines were involved in a disulfide bond in the folded protein, performed a trypsin digestion in both reducing and non-reducing conditions. The digestion products were then separated on a SDS-PAGE in non-reducing condition. The results reported in Fig. 7 showed that in presence of 1 mM DTT, GKN1 trypsin digested gave rise to two proteolytic products (17 and 11 kDa), whereas in absence of DTT it produced a band with the same molecular weight of undigested protein. These data indicated that the two proteolytic fragments were bound by a disulfide bond between Cys63 and one of the other three cysteine residues.

### 3.3 Fluorescence measurements

With the aim at investigate the stability of recombinant GKN1, toward chemical denaturants, protein fluorescence spectra were acquired either in the presence or in the absence of chemical denaturants. In general, wavelength of the maximum fluorescence intensity of aromatic residues has tendency to shift toward long wavelengths, when the aromatic residues present in hydrophobic regions become non exposed to polar environments. The results obtained reported in Fig. 8 and Fig. 9 indicated that GKN1 in the absence of denaturants showed a typical maximum fluorescence intensity at around 340 nm, characteristic of rather solvated aromatic residues. The addition of increasing concentration of Gdn-HCl promoted a quenching of the fluorescence intensity and a concomitant marked red shift of the maximum fluorescence.

The chemical denaturation profiles (Fig. 8B) evaluated either as variation of maximum fluorescence intensity at 343nm or shift of wavelength of the maximum fluorescence intensity at 343nm showed that the value of the denaturant concentration at half completion of the transition was 2.4 M for both

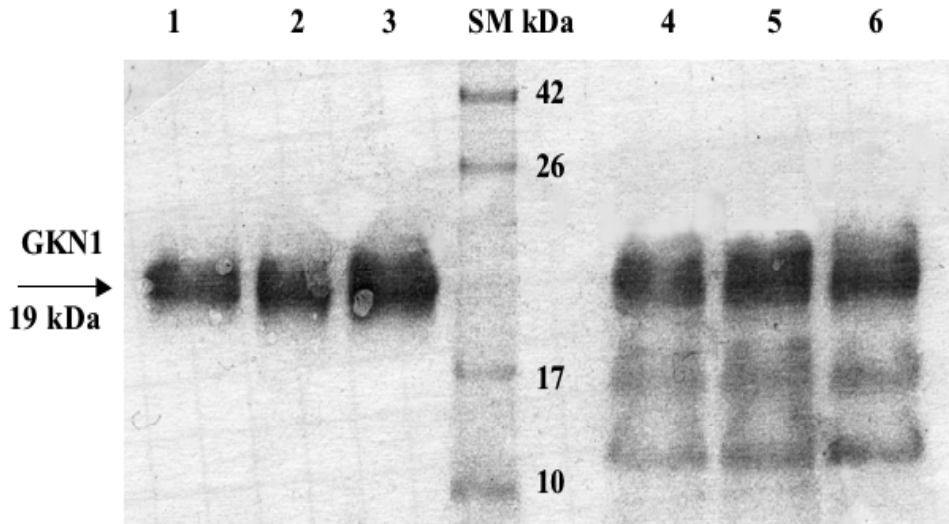


**Figure 7 Proteolysis of GKN1 in absence and presence of DTT**

GKN1 was incubated in the presence of trypsin and at the indicated times, sample aliquots were withdrawn from the reaction mixture and separated on non-denaturing SDS-PAGE. Lanes: 1-3, sample after 5, 10 and 15 minutes incubation in absence of DTT; 4 – 6, sample after 5, 10 and 15 minutes incubation in presence of DTT. SM, size marker

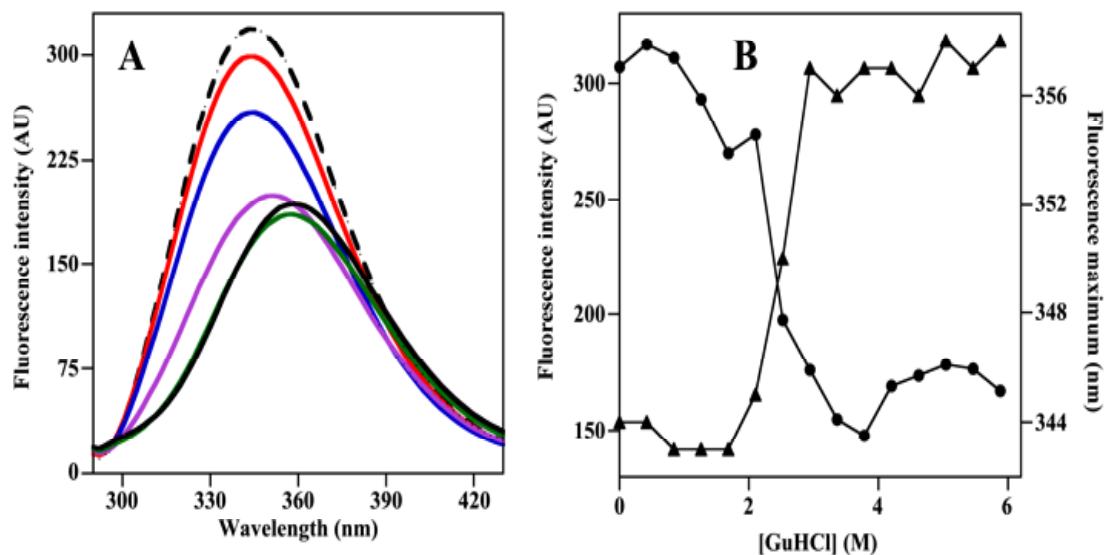


**Figure 8 Denaturation profile of GKN1 in guanidine-HCl**

A. Fluorescent emission spectra of GKN1 at increasing concentration of Gdn-HCl. The exciting wavelength was 280nm. The emission and excitation slits were set at 10nm. B.Variation of the maximum fluorescence intensity at 343 nm ( $\Delta$ ) and shift of the maximum fluorescence intensity ( $\bullet$ ) at increasing concentrations of Gdn-HCl.

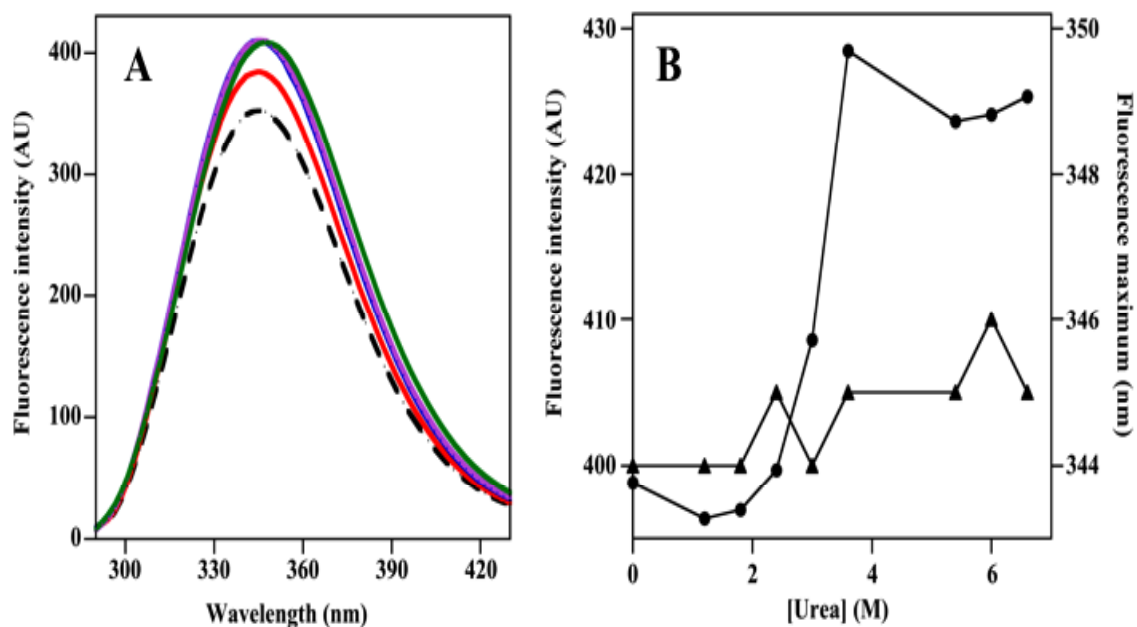


### Figure 9 Denaturation profile of GKN1 in urea

A. Fluorescent emission spectra of GKN1 at increasing concentration of urea. The exciting wavelength was 280nm. The emission and excitation slits were set at 10nm. B. Variation of the maximum fluorescence intensity at 343 nm ( $\Delta$ ) and shift of the maximum fluorescence intensity ( $\bullet$ ) at increasing concentrations of urea.

The behavior of the protein against urea denaturation was different. In fact, the fluorescence spectra of GKN1 at increasing concentration of urea showed only a small shift of the maximum fluorescence intensity and a concomitant progressive increase of fluorescence intensity (Fig. 9A). The value of the urea concentration at half completion of the transition was 3.8 M (Fig. 9B).

To evaluate the behavior of the protein in non-denaturing conditions, temperature melting profiles were recorded by fluorescence measurements. The heat denaturation profile at pH 6.5 showed a  $t_{1/2}$  of 70°C (Fig. 10A). However, the profile registered at different pH, indicated that the heat denaturation was pH – dependent. In fact, in the pH 5-8 interval,  $t_{1/2}$  increased as the pH increased (Fig.10B).

### **3.4 Circular dichroism measurements**

Secondary structure of recombinant GKN1 was investigated by means of CD in the far-UV region. Figure 11A shows the CD spectra of the intact GKN1 recorded in 20 mM phosphate buffer pH 8.5. The spectra recorded at 20°C shows an intense negative band below 240 nm that is indicative of a prominent content of  $\beta$  structure. From the analysis of the CD spectra with CDSSTR method the percentage of secondary structure found in recombinant GKN1 was calculated. As reported in Table 1, the helix, strand, turns and unordered structure were 15, 29, 23, and 33%, respectively. In addition, the difference between the experimental and reconstructed data of the CD spectra was negligible. From these data it emerges that GKN1 contain a higher percentage of  $\beta$ -strands with respect the  $\alpha$ -helix content.

**Table 1 Calculated Secondary Structure Fractions in GKN1**

Helix1	Helix2	Strand1	Strand2	Turns	Unordered
0.06	0.09	0.18	0.11	0.23	0.33

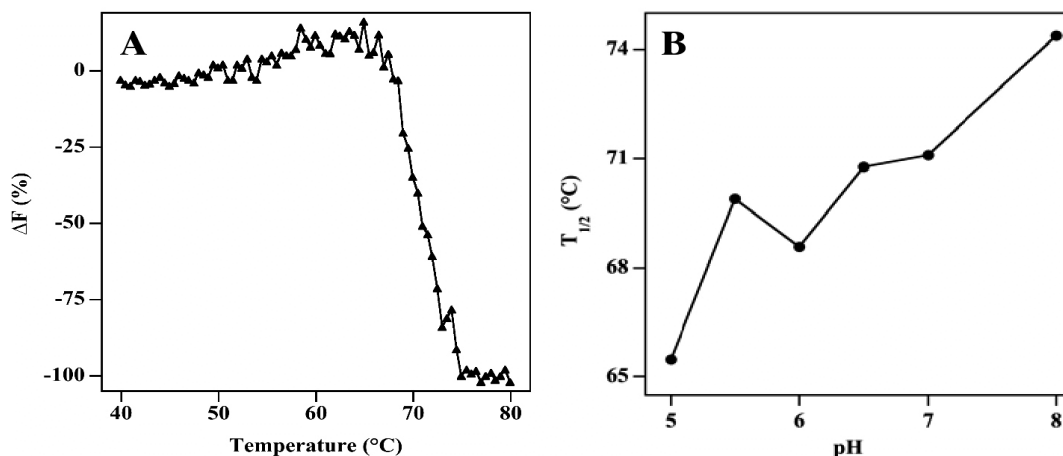


**Figure 10 Denaturation profile of GKN1 in non-denaturing conditions**

A. Temperature melting profile of GKN1 at pH 6.5 evaluated as percentage of fluorescence decrease at 340 nm. The exciting wavelength was 280nm. The emission and excitation slits were set at 10nm. The scan-rate was 0.2°C /min. B. Temperature melting ( $t_{1/2}$ ) evaluated at different pH.

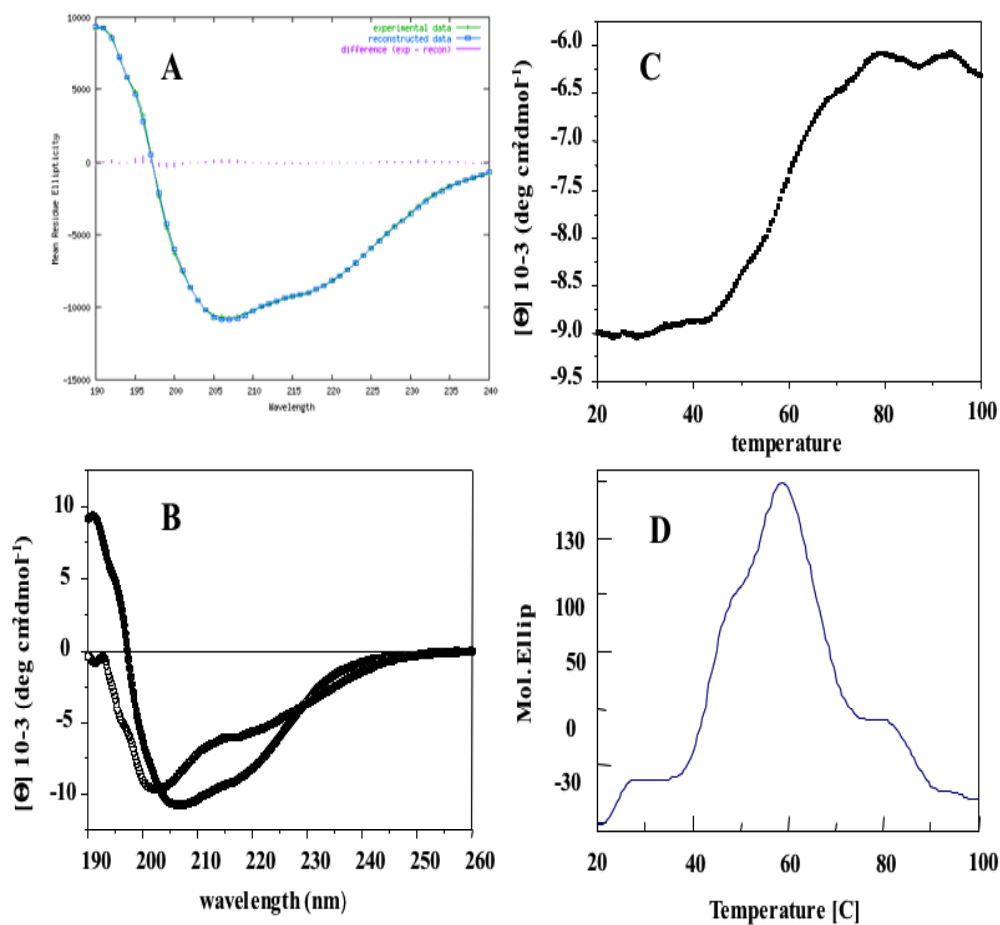


**Figure 11 CD spectra of GKN1 in the far UV**

A. CD spectra of native GKN1 at 20 °C, pH 8.5. B. CD spectra at 20°C (●) and 100 °C (○) . C. Variation of molecular ellipticity with temperature. D. First derivative of thermal denaturation profile of molecular ellipticity.

The CD profile taken at 100°C (Fig. 11B) shows the occurring of a transition in fact, a large band with a minimum around 200 nm is present thus indicating the formation of random coil structures. However, the CD profile still shows the presence of a rather large band above 200 nm thus indicating still the presence of residual secondary structure that could be due to the formation of soluble aggregates following thermal denaturation. To evaluate the thermal stability of the protein, CD denaturation curves were recorded in the temperature range 20 – 100 °C. The denaturation profile (Fig 11C) was obtained measuring the molecular ellipticity at 216 nm, corresponding to disappearance of helix content. The profile shows a flex around 59,5°C however, because the flex is not very sharp, the profile might suggest that the denaturation process occurs through several steps. In fact, the first derivative of the denaturation profile (Fig. 11D) indicated a major denaturation transition at 59.5°C and the presence of an additional transition at a lower temperature (47.5 °C). This transition appears irreversible because the CD spectra recorded at 20°C after thermal denaturation is not coincident to that recorded in the native condition (Fig. 11B).

Analysis of CD spectra in the near-UV region, recorded at 20°C and at 100°C are reported in Fig. 12A. The spectra at 20°C shows a more sharp band at 290 nm and a large band at 270 nm. The presence in this spectral region of these defined bands were indicative of a well defined ternary structure of the recombinant GKN1. However, both bands disappeared when the spectra were recorded at 100°C. This behaviour clearly indicated that at 100°C the tertiary structure of the protein is completely lost. The near-UV denaturation profile evaluated at 290 nm in the temperature interval 10-100°C (Fig. 12B) indicated the presence of two transition events, one occurring around 55°C and a second one at 77°C. These data suggest that the protein is endowed of two distinct domains that follow an independent thermal denaturation process.

Evaluation of the calorimetric properties of GKN1 was determined in 20 mM phosphate buffer pH 8.5 by differential scanning calorimetry (DSC) and the results obtained (Fig. 13) were similar to those obtained from near-UV. In fact, the DSC profile is quite broad showing a pick around 59.5°C and a large shoulder around 75°C.

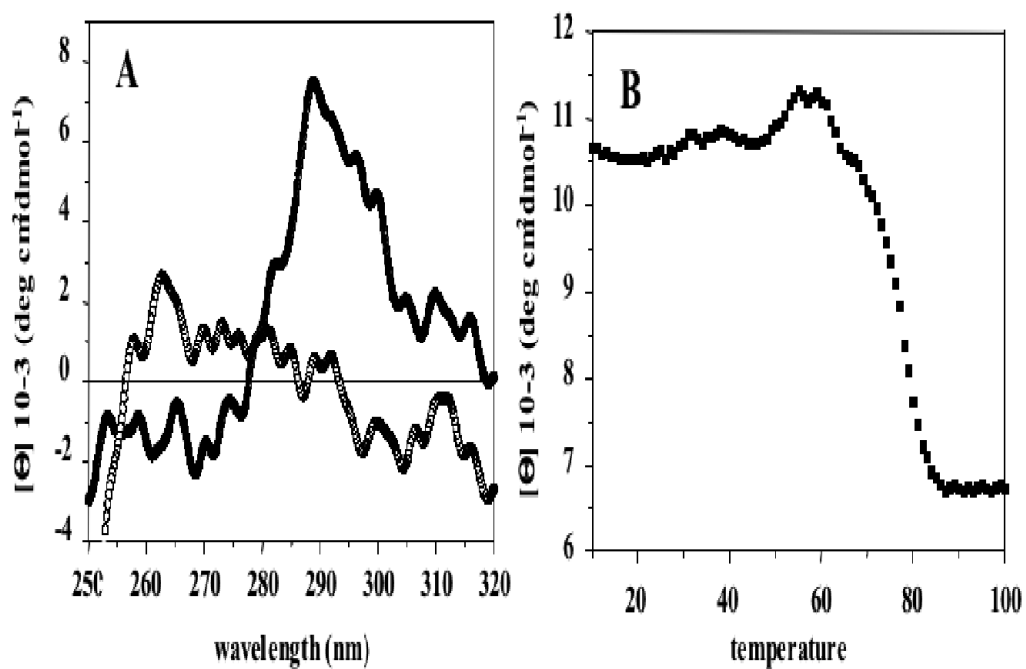


**Figure 12 CD spectra of GKN1 in the near UV**

A. CD spectra of native GKN1 at 20 °C, pH 8.5 (•) and of GKN1 at 100 °C (○). B. Variation of molecular ellipticity with temperature.

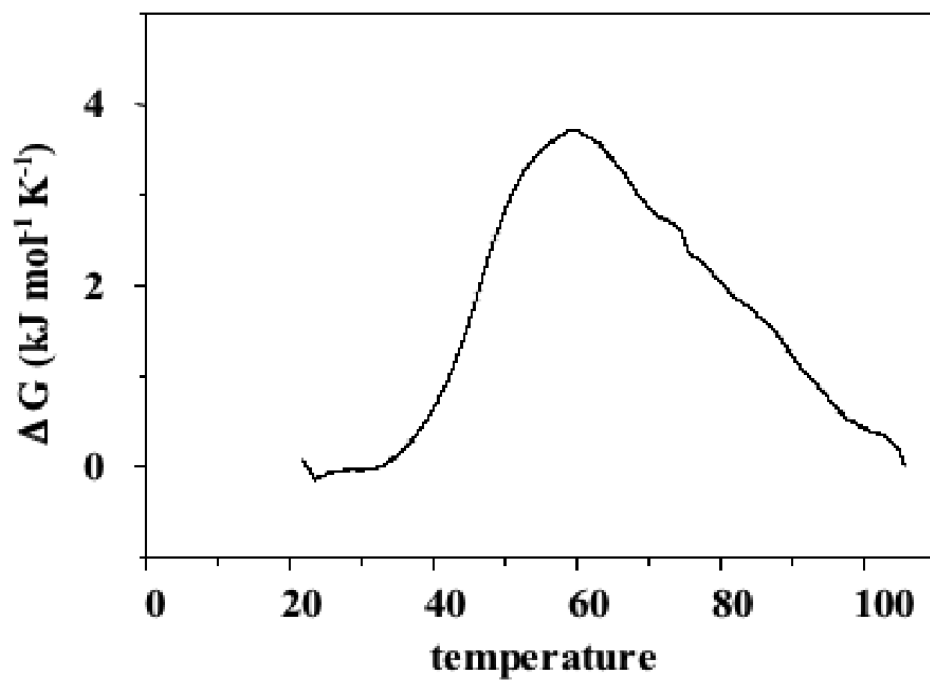


Figure 13 Differential scanning calorimetry (DSC) of GKN1

### 3.5 GKN1 secondary structure prediction and 3D modelling

Bioinformatic tools to predict the secondary structure of recombinant GKN1 were used to establish whether it would be closer to that determined by CD spectroscopy. To this purpose, the amino acid sequence of the expressed protein (Fig. 6A) was used as template. Psipred Server generated a scheme (Fig. 14) showing the distribution of secondary structural elements within GKN1 sequence from which it was calculated that the content of  $\alpha$ -helices and  $\beta$ -sheet was 13.9 and 29.6%, respectively, values very close to those obtained by CD spectroscopy (see Table 1). Furthermore, using the same sequence, a 3D model of GKN1 was generated through Tasser Bioinformatic Server. A 3D model of GKN1 was predicted on the basis of known structure of proteins showing segments of their sequence with a similar secondary structural arrangement. Five possible pdb model files were generated with a C-score higher than  $-5.2$ . Among these models the one with C-score of  $-4.34$  was chosen as possible GKN1 3D model (Fig. 15) because its content of  $\alpha$ -helix and  $\beta$ -sheet was closer to those represented in Fig. 14.

### 3.6 Biological activity of GKN1

The data above reported clearly indicated that recombinant GKN1 was characterized by the presence of both secondary and tertiary structure, thus suggesting at least a correct folding of the protein. Because GKN1 has been reported to affect cell viability, to assess if recombinant GKN1 was also biologically active, the ability to affect cell proliferation *in vivo* using different cell cultures at different dosage of GKN1 was evaluated. The results (Fig. 16A) showed that GKN1 was endowed by anti-proliferation effect at a concentration of  $0.5 \mu\text{M}$  already after 24 hours of treatment of a human gastric carcinoma (AGS) and a human lung epidermid cancer (HI355) cell lines. The effect was dependent by the concentration of the protein since the inhibition of cell growth was higher at higher GKN1 concentration. A less marked effect was instead observed using human embryonic kidney 293 (HEK 293) cell line (Fig. 16B).



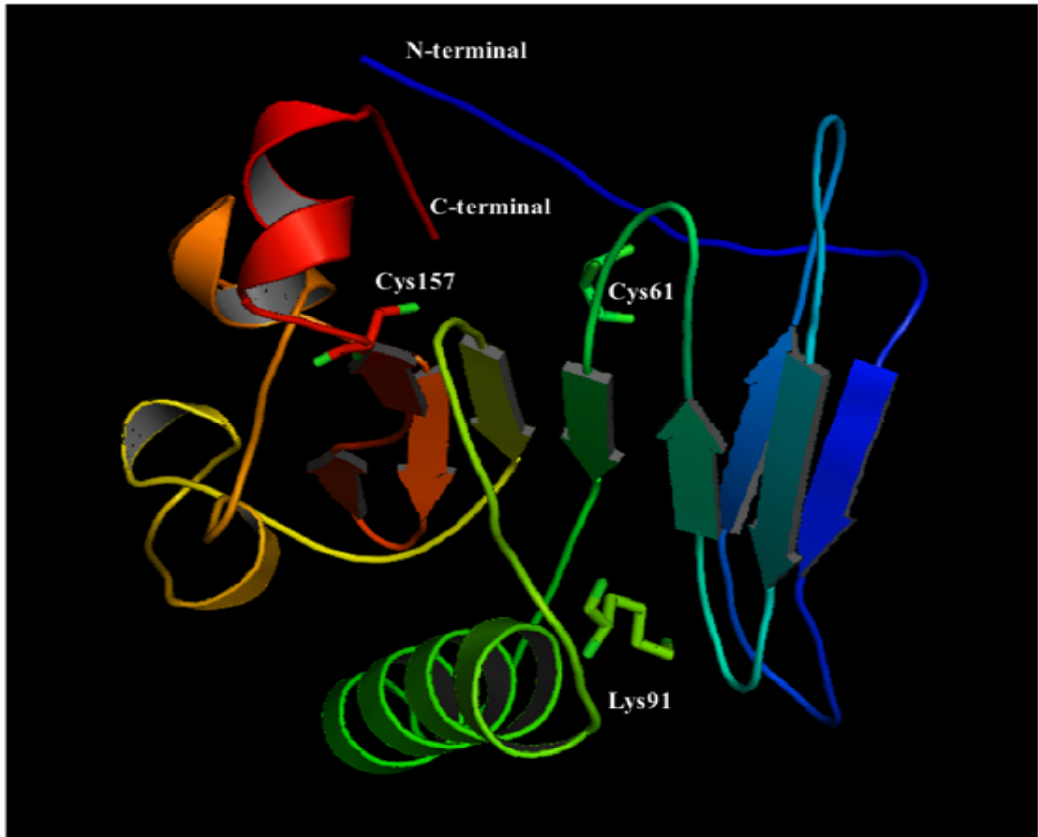


**Figure 15** 3D model of GKN1 built at the Tasser Bioinformatic Server. The position of the exposed Lys 91 and of the two closer cysteines or shown

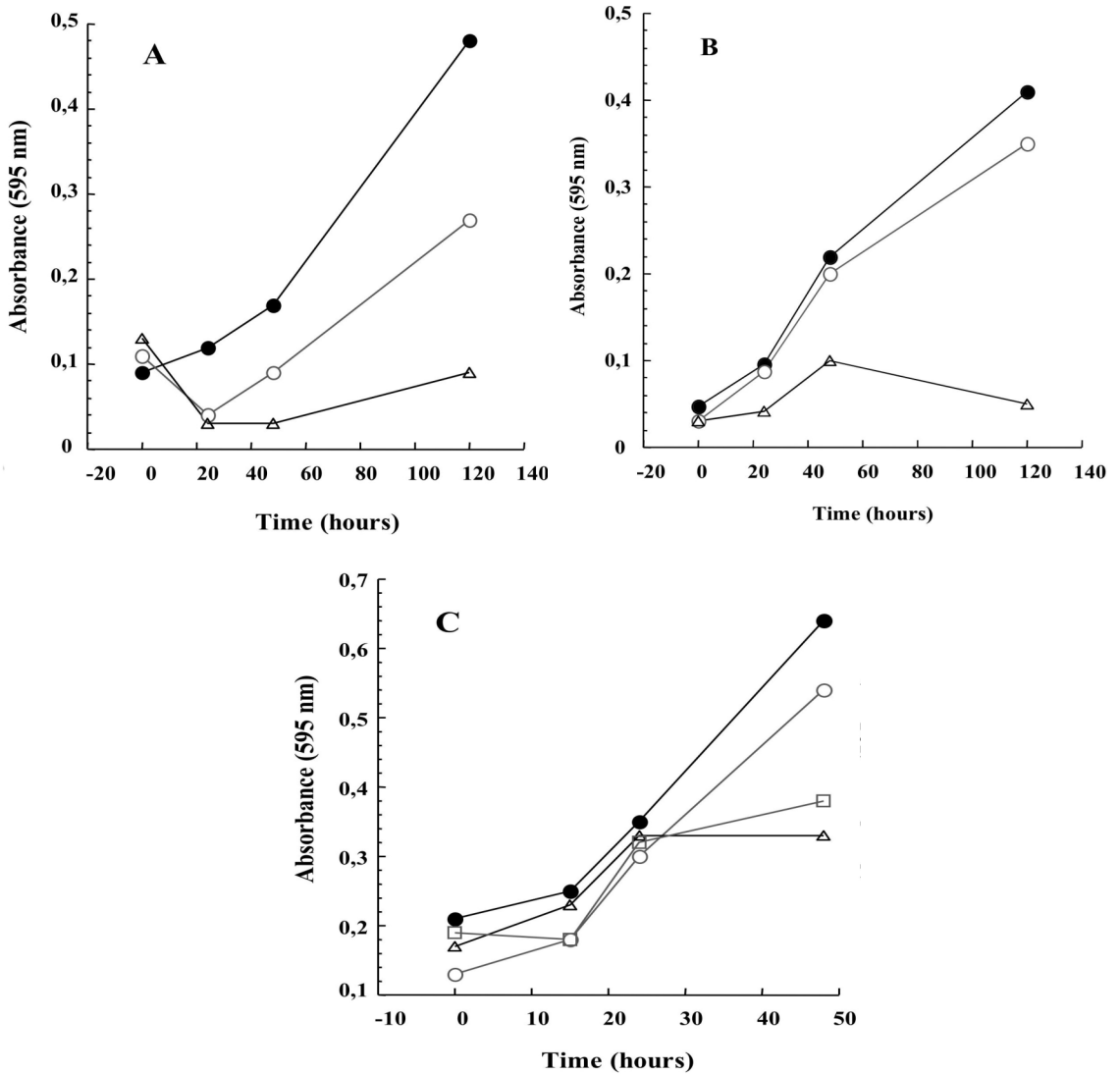


**Figure 16 Effect of GKN1 on cell growth**

A. AGS cell growth in absence (•) or in presence of 0.5  $\mu$ M (○) and 3  $\mu$ M (△) GKN1. B. H1355 cell growth in absence (•) or in presence of 0.5  $\mu$ M (○) and 3  $\mu$ M (△) GKN1. C. HEK293 cell growth in absence (•) or in presence of 5.5  $\mu$ M (○), 11  $\mu$ M (△) and 18  $\mu$ M (□) GKN1.

## DISCUSSION/CONCLUSIONS

In this study, the structural and biochemical properties of recombinant human GKN1 produced in yeast *Pichia pastoris* were investigated. The use of yeast system for protein expression was suggested by previous experiments where the expression of the GKN1 in heterologous *Escherichia coli* always gave a product that accumulated into inclusion bodies, even if the expression was carried out at 15°C (data not shown). All the attempts to refold the protein from inclusion bodies were unsuccessful. By contrast, the expression of GKN1 in yeast allowed obtaining purified soluble GKN1 at high yield.

The finding that the protein produced in yeast was soluble in water suggested that recombinant GKN1 possesses a certain level of structural organization. To investigate the structural features of the protein, its biochemical and spectroscopic properties were analyzed. Limited proteolysis indicated that the protein was moderately resistant toward proteases. In fact, time-course reactions with three proteases (trypsin, chymotrypsin and thermolysin) showed only a partial degradation of the protein. Protease resistance was also reported for GKN1 purified from chicken gizzard smooth muscle (21). However, in the latter case, the protein was cleaved by trypsin only at its N-terminal giving rise to a 18 kDa resistant core protein, in agreement to evidence that some proteins containing the BRICHOS domain are similarly cleaved (22-23). Because GKN1 is highly expressed in human normal stomach mucosal antrum, and thus exposed to a harsh environment, characterized by low pH and the presence of proteolytic enzymes (pepsin), its stability against enzyme degradation is highly required.

Moreover, the protein appears to be stabilized by the presence of a disulfide bridge most likely occurring between Cys63 and one of the other three Cys (Cys124, Cys147 and Cys161). No finding is reported up to now concerning the involvement of GKN1 cysteines in the interaction with other partner proteins, as instead it occurs between the homologous human GKN2 and TFF1 bounded through a disulfide bridge (30). However, GKN2 contains an additional cysteine residue (with respect to GKN1) that could be involved in this interaction (31).

The fluorescence properties of native GKN1 showed a  $\lambda_{\text{max}}$  fluorescence intensity at 340 nm which is characteristic of proteins with non tight globular structure. Generally globular proteins show fluorescence  $\lambda_{\text{max}}$  at a wavelength below 335 nm (32). The fluorescence spectra in the presence of guanidine suggested that recombinant GKN1 was correctly folded because a red shift was observed upon the addition a Gdn-HCl; This finding was indicative of a progressive exposure of aromatic amino acid residues. In addition, since increasing intensity of the fluorescence emission was observed only at Gdn-HCl concentration higher than 2.4 M, we supposed that the denaturation pathway of GKN1 occurs through the formation of an intermediate state. The fluorescence spectra acquired at increasing concentrations of urea showed a very small red shift with a continuous increasing of the fluorescence intensity, thus suggesting that the structure of GKN1 does not possess a hydrophobic globular core.

Moreover, the differences of GKN1 fluorescence profiles in Gdn-HCl and urea suggested that the protein was more stabilized by electrostatic interactions rather than hydrophobic ones. Thus, the ionic nature of Gdn-HCl masks electrostatic interactions in GKN1, a phenomenon that was absent when the uncharged urea was used. Although the difference in the ionic character should be the relevant factor in the denaturation process, the stability of GKN1 against Gdn-HCl suggests that the contribution of salt bridges to its stability may be limited. In this case, the fluorescence transition curves indicated that  $[\text{urea}]_{1/2} / [\text{Gdn-HCl}]_{1/2}$  was about two suggesting that Gdn-HCl has a stronger denaturing activity against GKN1. In conclusion, these results suggested a different unfolding pathways and mechanisms for the two denaturants. The following scheme (Fig. 17) represents the two possible unfolding pathways in Gdn-HCl and urea solutions for human recombinant GKN1. (33). The results from CD spectroscopy highlighted that GKN1 has a content of  $\beta$ -structures higher than  $\alpha$ -helix, and only 33% of the protein contains random coils.



These structural data are in agreement with predictions of secondary structure made for proteins containing the BRICHOS domain, and in particular with that of gastrophilin family (34).

Most BRICHOS proteins have four regions: hydrophobic, linker, BRICHOS and C-terminal domains. The hydrophobic region is often a trans-membrane segment (predictions and 35) included in the signal peptide for GKN1 and GKN2 (36). GKN1 and GKN2 may have a central natively disordered segment corresponding with a strongly predicted coiled segment. This was surprising since this characteristic was not shared by the others BRICHOS-protein family (34).

A prediction of the secondary structure of GKN1 made by the PSIPRED Protein Structure Prediction Server showed that it was consistent with the secondary structure predicted on the basis of CD spectroscopy (Fig. 14). In fact, the content of  $\beta$ -sheet and  $\alpha$ -helix was 33.3%, 14.5%, respectively, and such values are very similar to those predicted by the analysis of the CD spectra of the native protein. In particular, the CD profile is quite similar to that of  $\beta$ I-proteins showing a positive band around 190 nm with a negative shoulder around 220 nm (29). Furthermore, the CD melting profiles in the far and near-UV as well as in DSC measurement indicated that the protein was most likely characterized by the presence of two structural domains: one domain was more sensitive to physical and chemical denaturation and another one more resistant to denaturation, these domains corresponding, respectively, to the lower and higher DSC transitions.

Finally, with the purpose to construct a possible tertiary model structure of the recombinant GKN1, the bioinformatic program offered by the Tasser Server (Center for Computational Medicine and Bioinformatics, University of Michigan) was used. The model obtained predicted the structure of GKN1 on the base of sequence alignments with proteins of known 3D structure showing sequence similarity in small regions of the protein (Fig.15). The model is coherent with the content of  $\beta$ -sheet and  $\alpha$ -helix predicted by PSIPRED Protein Structure Prediction Server. From this model it is possible to highlight that at least Cys61 is close to Cys157 justifying the experimentally predicted disulfide bridge. Furthermore, the model clearly shows that the Lys 91 is very accessible to trypsin cleavage

## *Discussion*

---

in agreement to the proteolytic results. Moreover, the 3D model of GKN1 is in agreement with the spectroscopic data suggesting the presence of two distinct domains in the protein. The recombinant GKN1 showed also an antiproliferative effect on cancer cell lines. This result confirms the proposed protection role of GKN1 toward early gastric mucosal inflammation and supports also the postulated role as tumor suppressor.

## *Discussion*

---

## REFERENCES

1. Deans, C., Yeo, M. S., Soe, M. Y., Shabbir, A., Ti, T. K., So, J. B. (2011) Cancer of the gastric cardia is rising in incidence in an Asian population and is associated with adverse outcome, *World J. Surg.* 35, 617-624.
2. Krejs, G. J. (2010) Gastric cancer: epidemiology and risk factors, *Dig. Dis.* 28, 600-603.
3. Bashash, M., Yavari, P., Hislop, T. G., Shah, A., Sadjadi, A., Babaei, M., Brooks-Wilson A., Malekzadeh R., Bajdik C. (2011) Comparison of two diverse populations, British Columbia, Canada, and Ardabil, Iran, indicates several variables associated with gastric and esophageal cancer survival, *J. Gastrointest. Cancer* 42, 40-45.
4. Forman, D., and Burley, V.J. (2006) Gastric cancer: global pattern of the disease and an overview of environmental risk factors, *Best Pract. Res. Clin. Gastroenterol.* 20, 633-649.
5. Pollock, J., and Welsh, J. S. (2011) Clinical cancer genetics: Part I: Gastrointestinal, *Am. J. Clin. Oncol.* 34, 332-336.
6. Ernst, P. (1999) Review article: the role of inflammation in the pathogenesis of gastric cancer, *Aliment. Pharmacol. Ther.* 13, 13-18.
7. Cavaleiro-Pinto, M., Peleteiro, B., Lunet, N., Barros, H. (2011) *Helicobacter pylori* infection and gastric cardia cancer: systematic review and meta-analysis, *Cancer Causes Control* 22, 375-338.
8. Correa, P. (1995) *Helicobacter pylori* and gastric carcinogenesis, *Am. J. Surg. Pathol.* 19, S37-S43.
9. Meining, A., Kompisch, A., Stolte, M. (2003) Comparative classification and grading of *Helicobacter pylori* gastritis in patients with gastric cancer and patients with functional dyspepsia, *Scand. J. Gastroenterol.* 38, 707-711.
10. Roukos, D. H. (2000) Current status and future perspectives in gastric cancer management. *Cancer Treat. Rev.* 26, 243-255.
11. Shiozaki, K., Nakamori, S., Tsujie, M., Okami, J., Yamamoto, H., Nagano, H., Dono, K., Umeshita, K., Sakon, M., Furukawa, H., Hiratsuka, M., Kasugai, T., Ishiguro, S., Monden, M. (2001) Human stomach-specific gene, CA11, is down-regulated in gastric cancer, *Int. J. Oncol.* 19, 701-707.

## References

---

12. Oien, K. A., McGregor, F., Butler, S., Ferrier, R. K., Downie, I., Bryce, S., Burns, S., Keith, W. N. (2004) Gastrokine 1 is abundantly and specifically expressed in superficial gastric epithelium, down-regulated in gastric carcinoma, and shows high evolutionary conservation, *J. Pathol.* 203, 789-797.
13. Martin, T. E., Powell, C. T., Wang, Z., Bhattacharyya, S., Walsh-Reitz, M. M., Agarwal, K., Toback, F. G. (2003) A novel mitogenic protein that is highly expressed in cells of the gastric antrum mucosa, *Am. J. Physiol. Gastrointest. Liver Physiol.* 285, G332-G343.
14. Nardone, G., Rippa, E., Martin, G., Rocco, A., Siciliano, R.A., Fiengo, A., Cacace, G., Malorni, A., Budillon, G., Arcari, P. (2007) Gastrokine 1 expression in patients with and without *Helicobacter pylori* infection, *Dig. Liver Dis.* 39, 122- 129.
15. Nardone, G., Martin, G., Rocco, A., Rippa, E., La Monica, G., Caruso, F., Arcari, P.(2008) Molecular expression of gastrokine 1 in normal mucosa and in *Helicobacter pylori*-related pre-neoplastic and neoplastic lesions, *Cancer Biol. Ther.* 7, 1890-1895.
16. Walsh-Reitz, M. M., Huang, E. F., Musch, M. W., Chang, E. B., Martin, T. E., Kartha, S., Toback, F. G. (2005) AMP-18 protects barrier function of colonic epithelial cells: role of tight junction proteins, *Am. J. Physiol. Gastrointest. Liver Physiol.* 289, G163-G171.
17. Rippa, E., La Monica, G., Allocca, R., Romano, M. F., De Palma, M., Arcari, P. (2011) Over-expression of gastrokine 1 in gastric cancer cells induces fas-mediated apoptosis, *J. Cell. Physiol.* 226, 2571-2578.
18. Moss, S. F., Lee, J. W., Sabo, E., Rubin, A. K., Rommel, J., Westley, B. R., May, F. E., Gao, J., Meitner, P. A., Tavares, R., Resnick, M. B. (2008) Decreased expression of gastrokine 1 and the trefoil factor interacting protein TFIZ1/GKN2 in gastric cancer: influence of tumor histology and relationship to prognosis, *Clin. Cancer Res.* 14, 4161-4167.
19. Yoshikawa, Y., Mukai, H., Hino, F., Asada, K., Kato, I. (2000) Isolation of two novel genes, down-regulated in gastric cancer, *Jpn. J. Cancer Res.* 91, 459-463.

## References

---

20. Kozak, M. (1987) An analysis of 5'-noncoding sequences from 699 vertebrate messenger RNAs, *Nucleic Acids Res.* 15, 8125-8148.
21. Hnia, K., Notarnicola, C., de Santa Barbara, P., Hugon, G., Rivier, F., Laoudj-Chenivresse, D., Mornet, D. (2008) Biochemical properties of gastrokine-1 purified from chicken gizzard smooth muscle, *PLoS One* 3, e3854.
22. Sanchez-Pulido, L., Devos, D., Valencia, A. (2002) BRICHOS: a conserved domain in proteins associated with dementia, respiratory distress and cancer, *Trends Biochem. Sci.* 27, 329-332.
23. Willander, H., Hermansson, E., Johansson, J., Presto, J. (2011) BRICHOS domain associated with lung fibrosis, dementia and cancer - a chaperone that prevents amyloid fibril formation, *FEBS J.* 278, 3893-3904.
24. Sambrook et al.: *Molecular Cloning. A Laboratory Manual*, 2nd ed. Cold Spring Harbor Laboratory Press, Cold Spring Harbor, NY, 1989.
25. Lowry, O. H., Rosebrough, N. J., Farr, A. L., Randall, R. J. (1951) Protein measurement with the Folin phenol reagent. *J. Biol. Chem.* 193, 265-275.
26. Gill, S. C., and von Hippel, P. H. (1989) Calculation of protein extinction coefficients from amino acid sequence data, *Anal. Biochem.* 182, 319-326.
27. Compton, L. A., and Johnson, W.C. Jr. (1986) Analysis of protein circular dichroism spectra for secondary structure using a simple matrix multiplication, *Anal. Biochem.* 155, 155-167.
28. Whitmore, L., and Wallace, B.A. (2004) DICHROWEB: an online server for protein secondary structure analyses from circular dichroism spectroscopic data, *Nucleic Acids Res.* 32, 668-673.
29. Sreerama, N., and Woody R.W. (2000) Estimation of protein secondary structure from circular dichroism spectra: comparison of CONTIN, SELCON, and CDSSTR methods with an expanded reference set, *Anal. Biochem.* 287, 252-260.
30. Westley, B. R., Griffin, S. M., May, F. E. (2005) Interaction between TFF1, a gastric tumor suppressor trefoil protein, and TFIZ1, a brichos

- domain-containing protein with homology to SP-C, *Biochemistry* 44, 7967-7975.
31. Kouznetsova, I, Laubinger, W., Kalbacher, H., Kalinski, T., Meyer, F., Roessner, A., Hoffmann W. Biosynthesis of gastroke-2 in the human gastric mucosa: restricted spatial expression along the antral gland axis and differential interaction with TFF1, TFF2 and mucins. *Cell Physiol Biochem.* 2007;20(6):899-908.
  32. Oscar, D. M., Cyrili, M. K., Robert, S. H.( 1994).Protein denaturation with guanidine hydrochloride or urea provides a different estimate of stability depending on the contributions of electrostatic interactions . *Protein science* 3: 1984-1991
  33. Fouzia, R., Sandeep, S., Bilqees, B., (2005). Comparison of Guanidine Hydrochloride (GdnHcl) and Urea Denaturation on inactivation and unfolding of human placental cystatin ( HPC). *Protein Journal* Vol. 24, No.5.
  34. Hedlund, J., Johansson, J., Persson, B. (2009) BRICHOS - a superfamily of multidomain proteins with diverse functions. *BMC Res. Notes* 2, 180.
  35. Martin, L., Flihrer, R., Reiss, K., Kremmer, E., Saftig, P., Haass, C., (2008) Regulated intramembrane proteolysis of Bri2 (Itm2b) by ADAMI0 and SPPL2a/SPPL2b. *J biolo chem.* 283(3) : 1644-1652
  36. Bairoch, A., Boeckmann, B.,Ferro, S.,Gasteiger, E.,: Swiss-Prot juggling between evolution and stability . *Brief bioinform* 2004, 5: 39-55